JCTC Journal of Chemical Theory and Computation

Letter

pubs.acs.org/JCTC

Fate of a Graphene Flake: A New Route toward Fullerenes Disclosed with Ab Initio Simulations

Fabio Pietrucci* and Wanda Andreoni*

Institut de Théorie des Phénomènes Physiques, Ecole Polytechnique Fédérale de Lausanne, Switzerland

Supporting Information

ABSTRACT: The top-down formation of a fullerene from a graphene flake is investigated via extensive *ab initio* molecular dynamics simulations in the range 300−3000 K, accelerated by metadynamics. Topological (SPRINT) coordinates are used to ensure a prejudice-free exploration of the free-energy surface and path collective variables to provide reliable free-energy barriers. The low-barrier zipping of the 2D nanoflake into a 3D nanocone is revealed as the early key transformation, mediated by a four-membered ring. Multiple-step pathways lead it toward different but always fully tricoordinated 0D closed cages. This scenario comprises several key chemical reactions characteristic of carbon at the nanoscale, as known from diverse experiments.

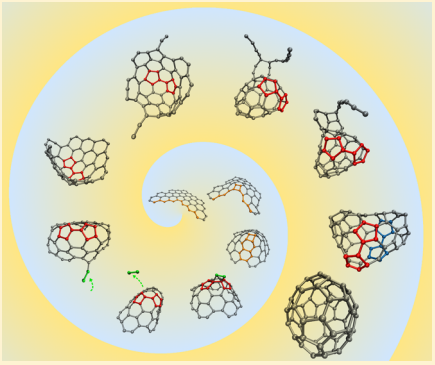

There is no doubt that graphitic carbon plays a leading role in the development of nanotechnology and nanoscience (see, e.g., refs 1−3). The unique chemical versatility of carbon allows for a multitude of spatial arrangements and functionalization and thus tremendously facilitates manipulation at the nanoscale and engineering of novel nanomaterials. The need to exploit these outstanding properties at best explains the paramount importance of understanding how and why certain carbon nanostructures form and transform under given physical and chemical conditions. In spite of remarkable successes of high-resolution transmission electron microscopy (HRTEM),[4−6] direct insight into the microscopic processes leading and accompanying their structural evolution remains a challenge.

The genesis of fullerenes is an outstanding example of such open intriguing issues. Although the 1985 discovery of C_{60} was the driving event in the nanocarbon era, the question "How does a fullerene cage form under given conditions?" has not found a compelling answer yet, from either experiment or modeling. Multiple and controversial hypotheses have long been formulated on bottom-up routes,[7−9] and only very recently experimental evidence has emerged for "a closed network growth" of fullerenes from carbon vapor via ingestion of carbon atoms or dimers.[10] On the contrary, the possibility of top-down formation from graphite sheets has long been considered marginal as an alternative process. The situation changed when, in 2010, in situ HRTEM[11] revealed the formation of a spheroidal carbon cage directly from graphene nanoflakes. Later, this was suggested to happen also in the interstellar medium under UV absorption.[12] The mechanisms however were not unveiled. The analysis of HRTEM aimed at inferring the transformation path, first followed a conventional procedure—using a few snapshots subjected to geometry optimization via quantum chemical calculations[11]—and lately adopted a combination of observations and classical molecular dynamics (MD).[13] Although the modeling started from different configurations for the flake, both studies considered the formation of pentagons at the edge by atom loss as the initial key step for the folding. Earlier, high-temperature classical MD[14] had instead attributed this key role to the presence of edge defects at high density.

In this letter, we explore whether and how a graphene nanoflake may close up into a seamless cage, as a result of thermal activation only, and examine which energy scales are involved. Our investigation is based on *ab initio* MD[15] and the metadynamics (MTD) technique[16] for sampling enhancement and for the reconstruction of the free-energy surface (FES). It relies on density-functional-theory in the Perdew−Burke−Ernzerhof (PBE)[17] approximation for the exchange-correlation functional and on norm-conserving pseudopotentials for the core−valence interaction. MTD benefits from two recently developed collective variables (CVs): (i) the social permutation-invariant (SPRINT) coordinates,[18] which are crucial for our purpose since they allow one to blindly explore complex multistep structural rearrangements, that is, without any conjecture on either the final products of a reaction or the transition and intermediate states along the pathway; and (ii) path CVs,[19] which are especially useful when initial and final states are known and as such help refining the calculation of free-energy barriers (FEBs). More details on the computational methods are given in the Supporting Information (SI).

By applying both methods in sequence, we discover and characterize unforeseen pathways leading a 2D graphene flake

Received: December 22, 2013
Published: February 11, 2014

   dx.doi.org/10.1021/ct401103p | *J. Chem. Theory Comput.* 2014, 10, 913−917

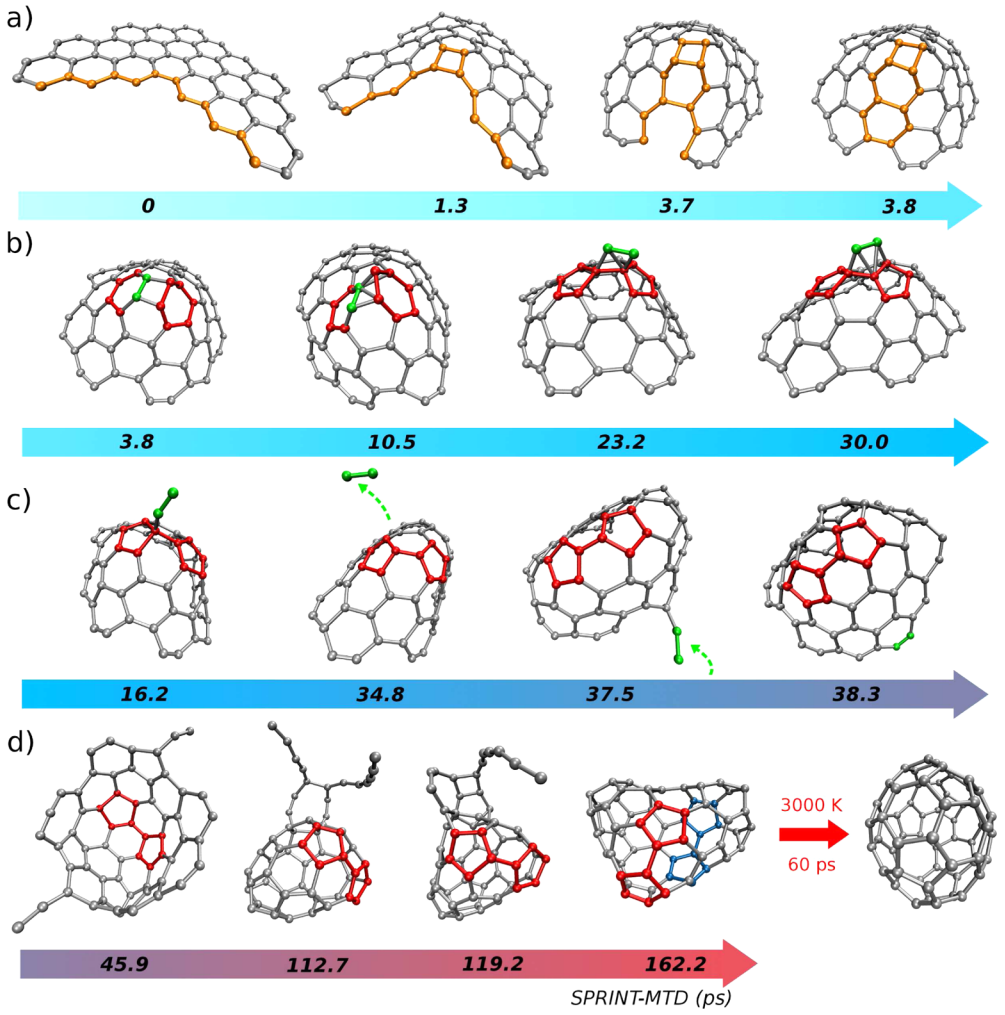

Figure 1. Structural evolution of a graphene nanoflake: (a–d) represent four important stages of the transformation. Time (in ps) refers to the 1000 K SPRINT-MTD simulation. The final structure is obtained upon heating at 3000 K (see text).

to 0D quasi-fullerenes, that is, fully tricoordinated closed cages.[20] In particular, we present evidence that loss of atoms is not necessary for the nanoflake to fold, but that it has a strong tendency to reshape into a nanocone with a four-membered ring (4MR) at the apex: This is the first key step toward thermally activated folding. Subsequent transformations are also identified: how pyracylenes (i.e., the building units of a fullerene) emerge in the interior of the nanocone, how edges reconstruct in analogy to a nanoribbon, and how short carbon chains rehybridize so as to drive the final closure of the cage.

The initial configuration of our simulations was a 60-atom fragment of graphene (Figure 1a) of shape closely reminiscent of the HRTEM flake image.[11] SPRINT-MTD was then applied and run a few times, under different conditions, at 300 K, 1000 K, and 2000 K, for a total duration of 700 ps. We shall describe an especially interesting and revealing set of simulations at 1000 K, in which the birth of a C_{60} fullerene is observed. The others will be discussed for the sake of comparison.

Key steps in the time evolution of the system at 1000 K are illustrated in Figure 1. The first transformation, from a 2D to a 3D structure, develops in an unforeseen way: a 4MR, more precisely a square, forms at the convex corner between two zigzag edges and induces their zipping, which in turn causes more hexagons to form and the flake to assume a pronounced conical shape (Figure 1a). Another very interesting process then takes place: the 4MR buckles, puckers and turns into a handle, based on a hexagon–hexagon junction, which eventually releases a dimer sticking on one atom. These changes at the apex of the cone are accompanied by the formation of a pyracylene subunit, namely one with two nonadjacent pentagons, each surrounded by hexagons only (Figure 1b). This structural motif is easily recognizable: it is the fingerprint of a nascent fullerene.[20]

As shown in Figure 1c, the C_2 unit finally desorbs from the cone apex but is recaptured from an armchair edge, thus creating a new hexagon at the border. In the following of the simulation, transformations at the edges continue to drive the global transformations of the carbon bowl. First, the bowl shrinks when carbon chains develop at the edges (Figure 1d), mainly stemming from pentagon vertices; then, as necklaces bridging across the orifice of the bowl, these chains become instrumental for its extension and closure. As shown in Figure 1d, chains born from a pentagon–pentagon junction rebind so as to form new rings including pentagons. Eventually, all are absorbed in a spheroidal (0D) tricoordinated cage, namely a quasi-fullerene.[20]

Further unbiased MD, heating the system up to 3000 K, was effective in removing some of the defects, thus lowering its potential energy by about 10 eV (see SI), but preserving some fused pentagons (Figure 1d). Continuing the simulation to

dx.doi.org/10.1021/ct401103p | J. Chem. Theory Comput. 2014, 10, 913–917

study pathways toward the icosahedral (I_h) C_{60} was outside the scope of this work. It is well-known indeed that there are 1812 unique fullerene isomers of I_h C_{60}[21] and that isomerization will involve several further costly steps, mainly releasing the strain induced by adjacent pentagons, each corresponding to a barrier in excess of 5 eV.[21−24] Also, it is fair to say that from the TEM images in ref 11. it is not possible to claim experimental evidence for either I_h C_{60} or even a fullerene, that is, a tricoordinated polyhedron with no polygons other than hexagons and 12 pentagons.

Our investigation focused then on understanding and quantitatively characterizing the key steps of the transformation. Unsaturated carbon dangling bonds at an open edge (see SI) make the flake prone to closure: this is the mechanism driving the formation of the 4MR (Figure 2). For

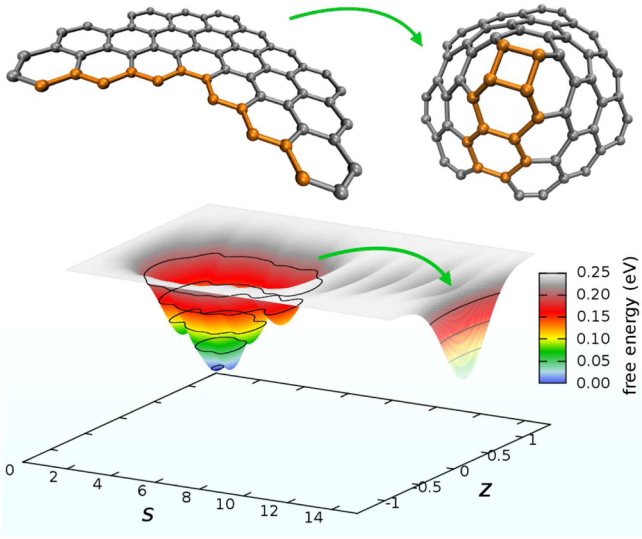

Figure 2. Graphene nanoflake: zipping into a nanocone and free-energy landscape as a function of the path collective variables.

this first closure event, we evaluated a relatively low (0.2 eV) and temperature independent FEB. The subsequent zipping into a cone was barrier-less. Indeed, in all our simulations, we did observe the nanocone to form readily and in the same sequence as mentioned above. A further unbiased Car−Parrinello MD, run for 30 ps at 1000 K, confirmed that the nanocone was a local minimum of the FES. For the sake of completeness, we also performed a geometry optimization: the cone-shaped configuration of the 60-atom fragment turned out to be energetically favored with respect to the planar structure of the 60-atom flake by 8.3 eV. This suggests that the reverse transformation, from the cone to the flake, is most likely irreversible.

Formation of the square deserves some more comments, because it is rather unusual for carbon. Indeed, it is a metastable configuration also in the route emerging from our simulations and, as such, does not survive our virtual synthesis of the cage. However, it is an important precursor. We emphasize that what we observe in our simulation, namely the development of pyracylene-like junctions from the square−hexagon junctions followed by the extrusion of a dimer, is the reverse transformation of what Rubin et al.[25] proposed already in 2000 for the synthesis of "nonclassical" C_{62} from C_{60}. Stable quasi-fullerenes incorporating 4MRs encircled by hexagons only have by now been synthesized.[26,27] More recently, this same structural motif has also emerged outside the fullerene world, namely in the synthesis of a (4)circulene (quadrannulene).[28]

Between two slightly different routes emerging from MTD for the formation of a (5665) pyracylene at the apex of the cone (Figure 3), path CV led to the one with the lowest FEB, which

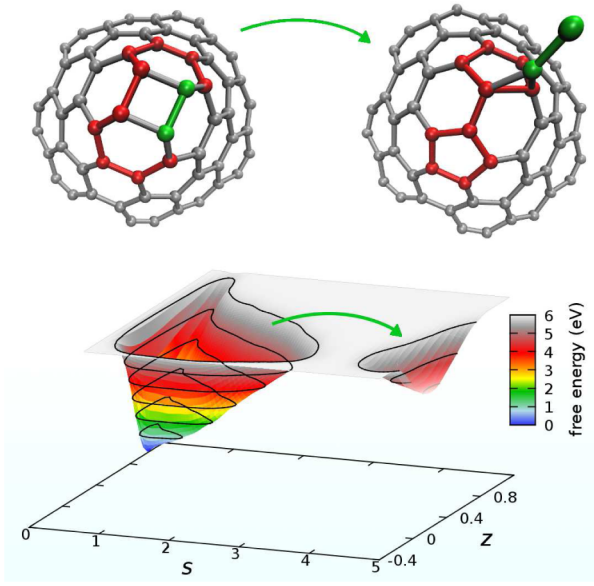

Figure 3. Formation of a pyracylene unit in the nanocone: free-energy landscape as a function of of the path collective variables.

turned out to be 6 eV, both at 300 K and at 1000 K. Remarkably, this is of the order of the energy barriers calculated for Stone-Wales transformations in Buckminsterfullerene[24] (7 eV at T = 0 K in calculations using the same PBE functional). The FEB for the subsequent ejection of the C_2 unit was 3 eV. These values could explain why we did not observe this reaction in three out of four simulations, although we did observe many attempts of the apex structure to reshape. In these cases, edge-driven processes intervened, such as local reconstruction of the rings or development of short sp chains, leading to the formation of pentagons, often adjacent, then moving from the periphery inward. In particular, we estimated a FEB of 0.95 eV for the (66) to (57) reconstruction at the nanocone zigzag edge: within the accuracy of the calculations, its value (at 300 K) is the same as the one we found for a graphene nanoribbon (GNR) of the same size (see SI). This result is consistent with the local character of this transformation and agrees with previous results on GNRs (see SI). While the GNR dynamics consists of repeated such transformations, with progressively lower barriers (see SI), the cones end up again into quasi-fullerenes, possessing corannulene sites, 4-, 7-, or 8-member rings but devoid of pyracylene units.

Our findings on the generation, ejection and recapturing of C_2 units might not be surprising: this scenario evokes the C_2 expulsion events observed in gas phase[29,30] and in MD simulations of the shrinking of hot giant fullerenes,[31−33] although they had a different role, happened at much higher temperatures and mainly from armchair edges or pentagons. Although one may argue that periodic boundary conditions help recapturing of a C_2 in the simulation (see SI), such events are likely also in the real system, given that carbon dimers are

dx.doi.org/10.1021/ct401103p | J. Chem. Theory Comput. 2014, 10, 913−917

likely products of the e-beam induced fragmentation of a graphene sheet.

The presence of floppy (also short) carbon chains at high temperatures is not an accident, as they are favored by entropic effects. Indeed, linear chains are observed ubiquitously during heat treatment of nanotubes[34] or at graphene contacts "in the presence of continuous energy input from the electron beam".[35] More interestingly, the evolution of (short) sp chains into sp^2 structures that we detect, finds confirmation in observations relative to the bottom-up formation of carbon nanostructures in hot plasma conditions[36,37] and in very recent NEXAFS experiments[38] on nanoparticles in the gas phase. The latter identified the predominant presence of linear chains and the sp-sp^2 transition already at low temperature. We notice that the sp chains appearing as tails in our simulation cannot be classified as either polyynes or cumulenes,[39,40] although closer to the latter, with a bond length alternation of 0.07 Å (corresponding to a bond order alternation of 0.6), and that they do not exhibit zigzag configurations.[35]

We then addressed the proposal of repeated losses of single carbon atoms as key steps driving the early formation of pentagons at the convex corner of the flake.[11] These events involve barriers for which no calculations are available. The only *ab initio* result reported[11] is a ∼5 eV energy difference for each desorption, which can be considered a lower limit to the barrier. By applying path-MTD, we made a few attempts to simulate the process proposed in ref 11, starting from the same 2D configuration of the 60-atom flake in Figure 1a, and also from a 62-atom-flake starting from Figure 1a after addition of an armchair edge. In both cases, our simulations failed to reproduce the atom desorption because of the occurrence, once more, of the zipping into a nanocone with the 4MR at the apex (Figure 2). These results further support the strong tendency of carbon nanoflakes to evolve into nanocones.

In conclusion, the results of the *ab initio* MD simulations presented here are consistent with the experimental observations in ref 11 and the suggestion of the top-down formation of a fullerene from graphene. In addition, they have revealed how a nanoflake can transform into a spheroidal carbon cage under thermal activation only, via a hitherto unforeseen sequence of events. These were obtained with a prejudice-free method that did not need any guess on either the final state or other configurations along the pathway.

In particular, the initial closure of the graphene flake into a nanocone via formation of a carbon square is found to happen at any temperature between 300 and 2000 K, with a relatively low free-energy barrier. This result does not obviously exclude the possibility that higher energy routes, such as atom loss, might be favored in laboratory experiments run at very high temperatures or under electron irradiation. On the other hand, the knowledge of the most facile path emerging from our study may prove to be relevant for process tailoring and optimization, and for avoiding degradation routes in graphene-based technology. Moreover, the existence of a nanocone and the pathway leading to it could be verified experimentally without the need of extreme conditions.

Another important message comes from the different dynamical behavior and energy scales pertaining to a nanoribbon, a convex nanoflake, and a nanocone of the same size. This emphasizes the strong dependence upon shape and termination, not only of their electronic properties at equilibrium but also of their fate under thermal treatment. In particular, the flake-cone transformation is facilitated by the presence of a corner between two intersecting zigzag edges.

We also remark that the scenario we observe for the top-down formation of a fullerene is consistent with many experimental observations and models for the bottom-up process: for example, the emerging of a pyracylene unit from a 4MR expelling a dimer is the inverted process of the synthesis route of C_{62} from C_{60}[25−27] and the carbon chains rehybridization, that allows for the final closure of the cage, is in agreement with the claimed accretion mechanism of carbon nanoparticles.[36−38] Moreover, the preceding step, namely the shrinking of the bowl, is reminiscent of the often proposed shrinking-wrap process of large cages toward smaller ones. This could indeed take place in conditions of high energy transfer leading to expulsion of the chain tails.

The use of the recently introduced SPRINT coordinates[18] in conjunction with *ab initio* metadynamics was the crucial advantage of our simulations. We believe that the robust methods we have used here not only allow to uncover the richness of chemistry at the nanoscale but open the way to new joint adventures of in-silico and laboratory experiments toward a rational design of graphene-based nanostructures.

■ ASSOCIATED CONTENT

Ⓢ Supporting Information

Here, we report on details of the methods employed, on the computational scheme, on our simulations of the edge reconstruction of a graphene nanoribbon, and also further corroborating results. This material is available free of charge via the Internet at http://pubs.acs.org.

■ AUTHOR INFORMATION

Corresponding Authors

*E-mail: fabio.pietrucci@epfl.ch.
*E-mail: wanda.andreoni@epfl.ch.

Author Contributions

The manuscript was written through contributions of both authors. Both authors have given approval to the final version of the manuscript.

Notes

The authors declare no competing financial interest.

■ ACKNOWLEDGMENTS

The computational work was supported as part of a CADMOS project. The financial support for CADMOS and for the Blue Gene/P system is provided by the Canton of Geneva, the Canton Vaud, the Hans Wilsdorf foundation, the Louis−Jeantet Foundation, the University of Geneva, the University of Lausanne, and the Ecole Polytechnique Fédérale de Lausanne.

■ REFERENCES

(1) *Carbon Nanotubes: Advanced Topics in the Synthesis, Structure, Properties and Applications*; Jorio, A., Dresselhaus, G., Dresselhaus, M., Eds.; Springer: Berlin and Heidelberg, 2008.
(2) Hirsch, A. *Nat. Mater.* **2010**, *9*, 868−871.
(3) Yang, H.; Heo, J.; Park, S.; Song, H. J.; Seo, D. H.; Byun, K.-E.; Kim, P.; Yoo, I.; Chung, H.-J.; Kim, K. *Science* **2012**, *336*, 1140−1143.
(4) Meyer, J. C.; Geim, A. K.; Katsnelson, M. I.; Novoselov, K. S.; Booth, T. J.; Roth, S. *Nature* **2007**, *446*, 60−63.
(5) Girit, C. O.; Meyer, J. C.; Erni, R.; Rossell, M. D.; Kisielowski, C.; Yang, L.; Park, C.-H.; Crommie, M. F.; Cohen, M. L.; Louie, S. G.; Zettl, A. *Science* **2009**, *323*, 1705−1708.

(6) Huang, J. Y.; Ding, F.; Yakobson, B. I.; Lud, P.; Qie, L.; Li, J. *Proc. Natl. Acad. Sci. U.S.A.* **2009**, *106*, 10103−10108.
(7) Smalley, R. E. *Acc. Chem. Res.* **1992**, *25*, 98−105.
(8) Curl, R. F.; Haddon, R. M. *Philos. Trans. R. Soc. London Ser. A* **1993**, *343*, 19−32.
(9) Goroff, N. S. *Acc. Chem. Res.* **1996**, *29*, 77−83.
(10) Dunk, P. W.; Kaiser, N. K.; Hendrickson, C. L.; Quinn, J. P.; Ewels, C. P.; Nakanishi, Y.; Sasaki, Y.; Shinohara, H.; Marshall, A. G.; Kroto, H. W. *Nat. Commun.* **2012**, *3*, 855−863.
(11) Chuvilin, A.; Kaiser, U.; Bichoutskaia, E.; Besley, N. A.; Khlobystov, A. N. *Nat. Chem.* **2010**, *2*, 450−453.
(12) Berné, O.; Tielens, A. G. G. M. *Proc. Natl. Acad. Sci. U.S.A.* **2012**, *109*, 401−406.
(13) Santana, A.; Zobelli, A.; Kotakoski, J.; Chuvilin, A.; Bichoutskaia, E. *Phys. Rev. B* **2013**, *87*, 094110−094117.
(14) Lebedeva, I. V.; Knizhnik, A. A.; Bagaturyant, A. A.; Potapkin, B. V. *Phys. E* **2008**, *40*, 2589−2595.
(15) Car, R.; Parrinello, M. *Phys. Rev. Lett.* **1985**, *55*, 2471−2474.
(16) Laio, A.; Parrinello, M. *Proc. Natl. Acad. Sci. U.S.A.* **2002**, *99*, 12562−12566.
(17) Perdew, J. P.; Burke, K.; Ernzerhof, M. *Phys. Rev. Lett.* **1996**, *77*, 3865−3868.
(18) Pietrucci, F.; Andreoni, W. *Phys. Rev. Lett.* **2011**, *107*, 085504−085507.
(19) Branduardi, D.; Gervasio, F. L.; Parrinello, M. *J. Chem. Phys.* **2007**, *126*, 054103−054112.
(20) Godly, E.; Taylor, R. *Pure Appl. Chem.* **1997**, *69*, 1411−1434.
(21) Walsh, T. R.; Wales, D. J. *J. Chem. Phys.* **1998**, *109*, 6691−6700.
(22) Yi, J.-Y.; Bernholc, J. *J. Chem. Phys.* **1992**, *96*, 8634−8636.
(23) Eggen, B. R.; Heggie, M.; Jungnickel, G.; Latham, C. D.; Jones, R.; Briddon, P. R. *Science* **1995**, *272*, 87−92.
(24) Bettinger, H. F.; Yakobson, B. I.; Scuseria, G. E. *J. Am. Chem. Soc.* **2003**, *125*, 5572−5580.
(25) Qian, W.; Bartberger, M.; Pastor, S.; Houk, K.; Wilkins, C.; Rubin, Y. *J. Am. Chem. Soc.* **2000**, *122*, 8333−8334.
(26) Qian, W.; Chuang, S.-C.; Amador, R. B.; Jarrosson, T.; Sander, M.; Pieniazek, S.; Khan, S. I.; Rubin, Y. *J. Am. Chem. Soc.* **2003**, *125*, 2066−2067.
(27) Hirsch, A.; Brettreich, M. *Fullerenes: Chemistry and Reactions*; Wiley, Weinheim, 2005.
(28) Bharat; Bohla, R.; Bally, T.; Valente, A.; Cyrański, M. K.; Dobrzycki, L.; Spain, S. M.; Rempała, P.; Chin, M. R.; King, B. T. *Angew. Chem., Int. Ed.* **2010**, *49*, 399−402.
(29) O'Brien, S. C.; Heath, J. R.; Curl, R. F.; Smalley, R. E. *J. Chem. Phys.* **1988**, *88*, 220−230.
(30) Radi, P. P.; Bunn, T. L.; Kemper, P. R.; Molchan, M. E.; Bowers, M. T. *J. Chem. Phys.* **1988**, *88*, 2809−2814.
(31) Irle, S.; Zheng, G.; Wang, Z.; Morokuma, K. *J. Phys. Chem. B* **2006**, *110*, 14531−14545.
(32) Huang, J. Y.; Ding, F.; Kun, J.; Yakobson, B. I. *Phys. Rev. Lett.* **2007**, *99*, 175503−175506.
(33) Saha, B.; Irle, S.; Morokuma, K. *J. Phys. Chem. C* **2011**, *115*, 22707−22716.
(34) Jinno, M.; Ando, Y.; Bandow, S.; Fan, J.; Yudasaka, M.; Iijima, S. *Chem. Phys. Lett.* **2006**, *418*, 109−114.
(35) Chuvilin, A.; Meyer, J. C.; Algara-Siller, G.; Kaiser, U. *New J. Phys.* **2009**, *11*, 083019−083028.
(36) Shvartsburg, A. A.; Hudgins, R. R.; Dugourd, P.; Gutierrez, R.; Frauenheim, T.; Jarrold, M. F. *Phys. Rev. Lett.* **2000**, *84*, 2421−2424.
(37) Yamaguchi, Y.; Colombo, L.; Piseri, P.; Ravagnan, L.; Milani, P. *Phys. Rev. B* **2007**, *76*, 134119−134125.
(38) Ravagnan, L.; Mazza, T.; Bongiorno, G.; Devetta, M.; Amati, M.; Milani, P.; Piseri, P.; Coreno, M.; Lenardi, C.; Evangelista, F.; Rudolf, P. *Chem. Commun.* **2011**, *47*, 2952−2954.
(39) Jin, C.; Lan, H.; Peng, L.; Suenaga, K.; Iijima, S. *Phys. Rev. Lett.* **2009**, *102*, 205501−205504.
(40) Ravagnan, L.; Manini, N.; Cinquanta, E.; Onida, G.; Sangalli, D.; Motta, C.; Devetta, M.; Bordoni, A.; Piseri, P.; Milani, P. *Phys. Rev. Lett.* **2009**, *102*, 245502−245505.